Electronic Supplementary Information (ESI)

Highly Efficient Transformation of Linear Poly(Phenylene Ethynylene)s into Zigzag-Shaped π-Conjugated Microporous Polymers through Boron-Mediated Alkyne Benzannulation

Yoshiaki Shoji,* Minsu Hwang, Haruka Sugiyama, Fumitaka Ishiwari, Kumiko Takenouchi, Ryota Osuga, Junko N. Kondo, Shigenori Fujikawa and Takanori Fukushima*

*To whom correspondence should be addressed.
E-mail: yshoji@res.titech.ac.jp (Y.S.), fukushima@res.titech.ac.jp (T.F)

Table of Contents

Supplementary Scheme.

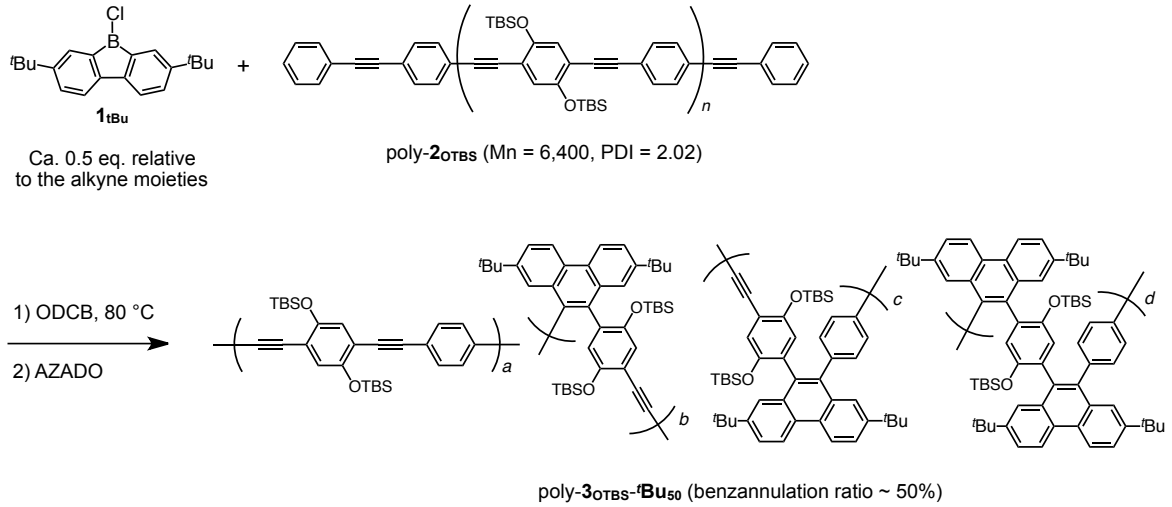

Scheme S1. Synthesis of poly-$\mathbf{3_{OTBS}}$-$^{t}\mathbf{Bu_{50}}$ from poly-$\mathbf{2_{OTBS}}$. Possible partial structures of poly-$\mathbf{3_{OTBS}}$-$^{t}\mathbf{Bu_{50}}$ are shown.

Supplementary Table.

Table S1. Molecular weight and PDI values of polymers, obtained by the SEC-MALS analysis.

Entry	Polymer	M_n / Da (SEC-MALS)	PDI (SEC-MALS)
1	poly-$\mathbf{3_{OTBS}}$-$^{t}\mathbf{Bu_{100}}$[a]	4.77 x 10^4 [c]	1.66
2	poly-$\mathbf{3_{OTBS}}$-$^{t}\mathbf{Bu_{50}}$[a]	1.62 x 10^4	1.52
3	poly-$\mathbf{3_{OTBS}}$-$\mathbf{H_{100}}$[a]	1.61x 10^4	1.34
4	poly-$\mathbf{3_{OHex}}$-$^{t}\mathbf{Bu}_{100}$	1.87 x 10^4 [c]	2.37
5	poly-$\mathbf{3_{OHex}}$-$\mathbf{H}_{100}$	2.25 x 10^4 [c]	2.00
6	poly-$\mathbf{3_{OTBS}}$-$^{t}\mathbf{Bu_{100}}$[b]	6.17 x 10^4 [c]	1.25
7	poly-$\mathbf{3_{OH}}$-$^{t}\mathbf{Bu_{100}}$[b]	1.28 x 10^5 [c]	1.14

[a]Synthesized from poly-$\mathbf{2}_{\mathrm{OTBS}}$ (M_{n} = 6,400, PDI = 2.02). [b]Synthesized from poly-$\mathbf{2}_{\mathrm{OTBS}}$ (M_{n} = 5,900, PDI = 2.32). [c]The values may be overestimated to some extent due to the occurrence of polymer aggregation in the SEC analysis.

Supplementary Figures.

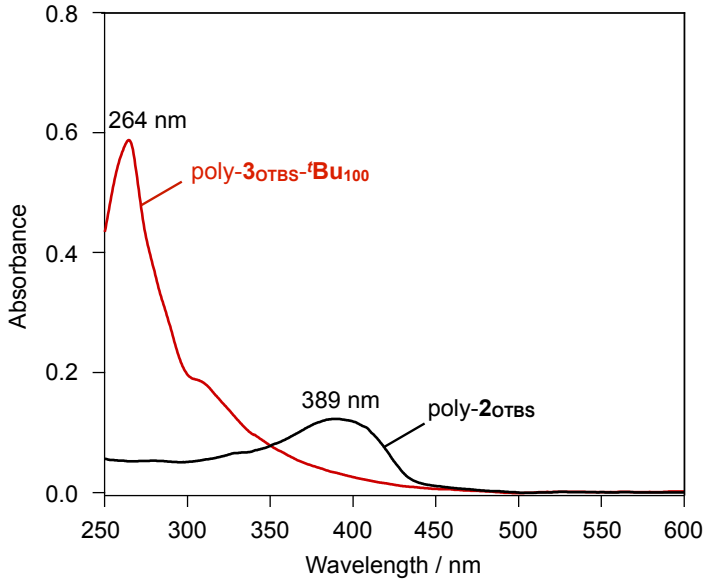

Fig. S1. Electronic absorption spectra of poly-**2**$_{\mathbf{OTBS}}$ (black, 3.2 x 10^{-3} mg mL^{-1}) and poly-**3**$_{\mathbf{OTBS}}$-^{t}**Bu**$_{\mathbf{100}}$ (red, 3.2 x 10^{-3} mg mL^{-1}) in CH_2Cl_2 at 25 °C.

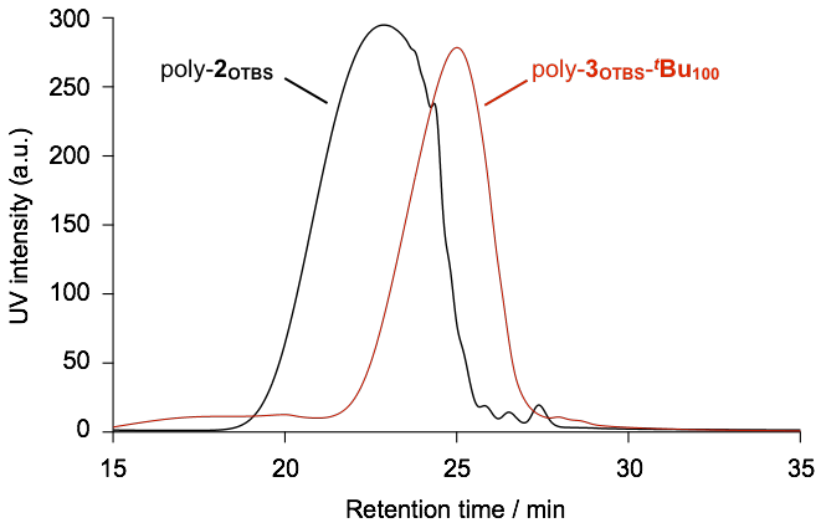

Fig. S2. GPC profiles of poly-**2**$_{\mathbf{OTBS}}$ (M_n = 6,400 Da, PDI = 2.02) and poly-**3**$_{\mathbf{OTBS}}$-^{t}**Bu**$_{\mathbf{100}}$ (eluent: $CHCl_3$).

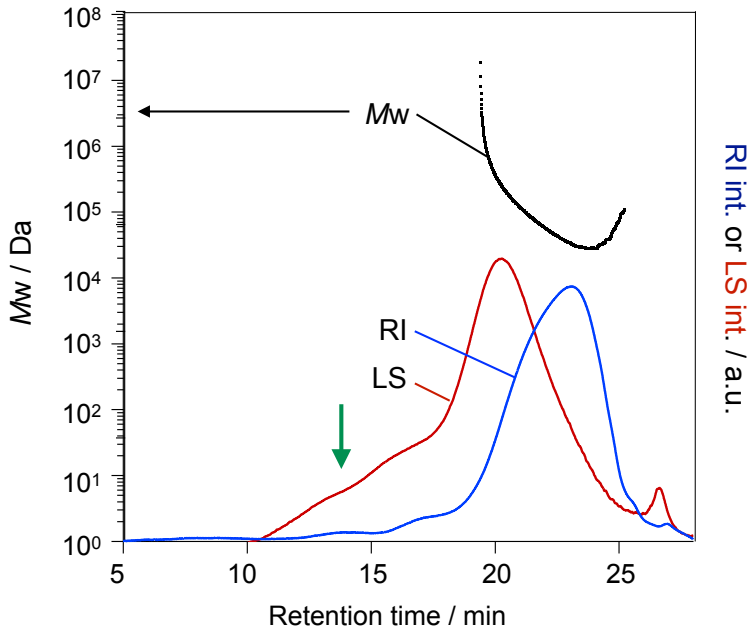

Fig. S3. SEC-MALS profile of poly-$\mathbf{3_{OTBS}}$-$^{t}\mathbf{Bu_{100}}$ (M_n = 4.77 x 10^4 Da, PDI = 1.66). The observed rise in the light-scattering (LS) trace (green arrow) suggests the occurrence of polymer aggregation in the SEC analysis, which may lead to the overestimation of the molecular weight of the polymer.

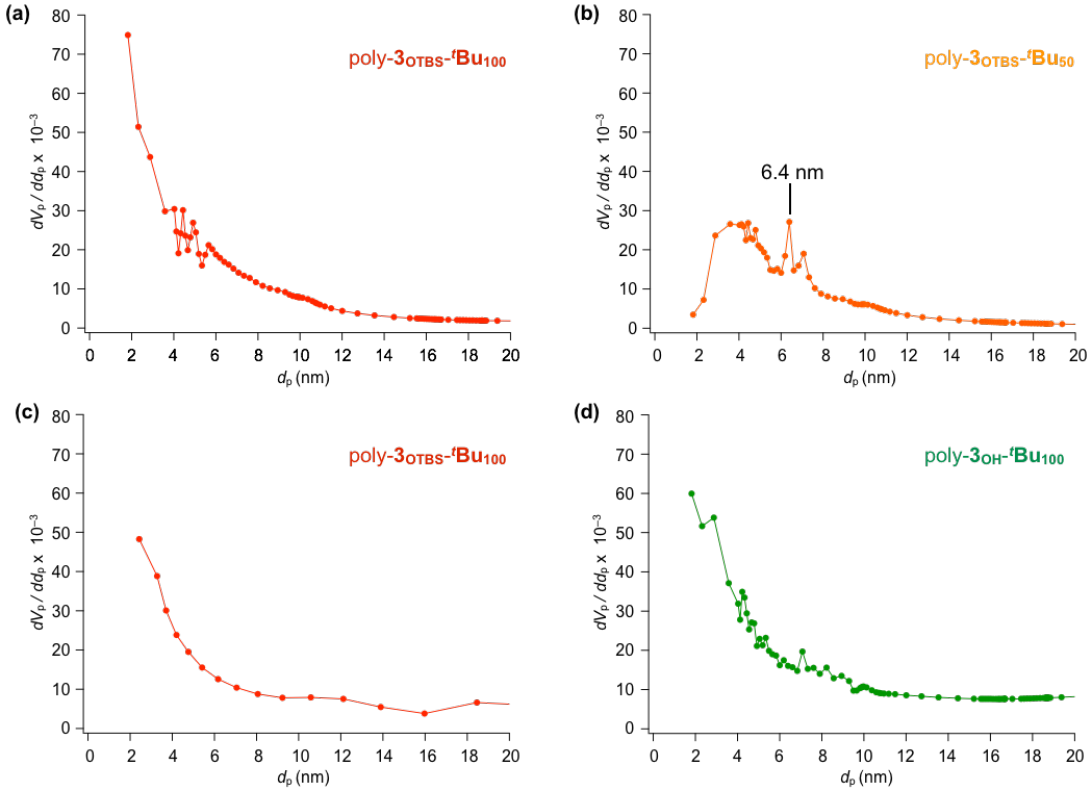

Fig. S4.BJH pore size distribution profiles of powder samples of (a) poly-$\mathbf{3_{OTBS}}$-$^{t}\mathbf{Bu_{100}}$ and (b) poly-$\mathbf{3_{OTBS}}$-$^{t}\mathbf{Bu_{50}}$ obtained from **poly-2$_{OTBS}$** (M_n = 6,400, PDI = 2.02), and (c) poly-$\mathbf{3_{OTBS}}$-$^{t}\mathbf{Bu_{100}}$ and (d) poly-$\mathbf{3_{OH}}$-$^{t}\mathbf{Bu_{100}}$ obtained from **poly-2$_{OTBS}$** (M_n = 5,900, PDI = 2.02).

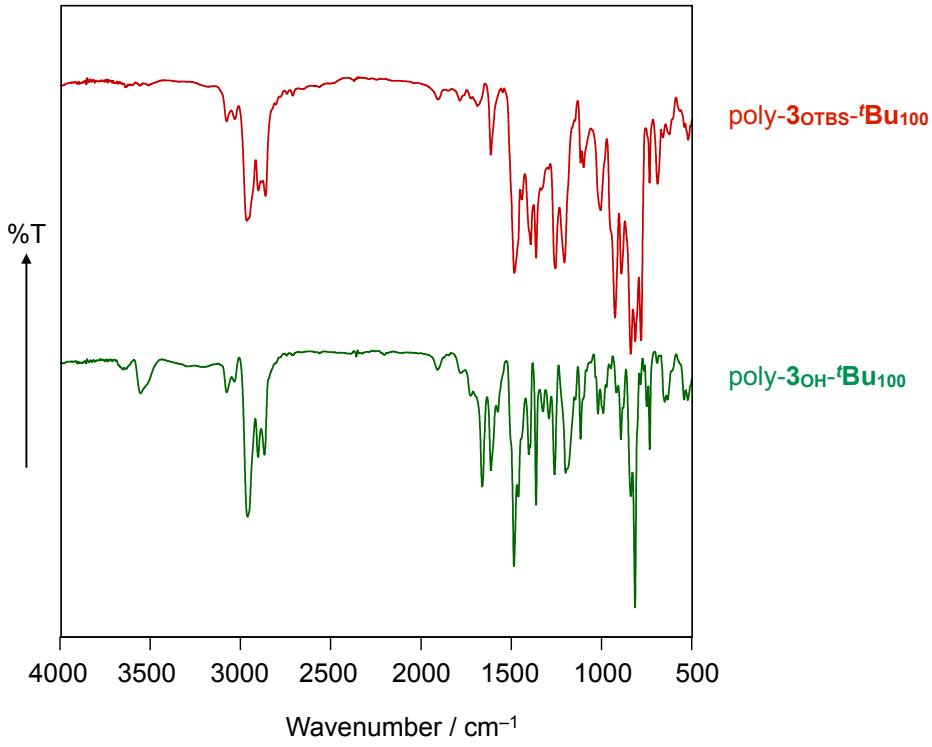

Fig. S5. IR spectra (KBr) of poly-$\mathbf{3_{OTBS}}$-$^{t}\mathbf{Bu_{100}}$ (red) and poly-$\mathbf{3_{OH}}$-$^{t}\mathbf{Bu_{100}}$ (green) at 25 °C

Analytical Data

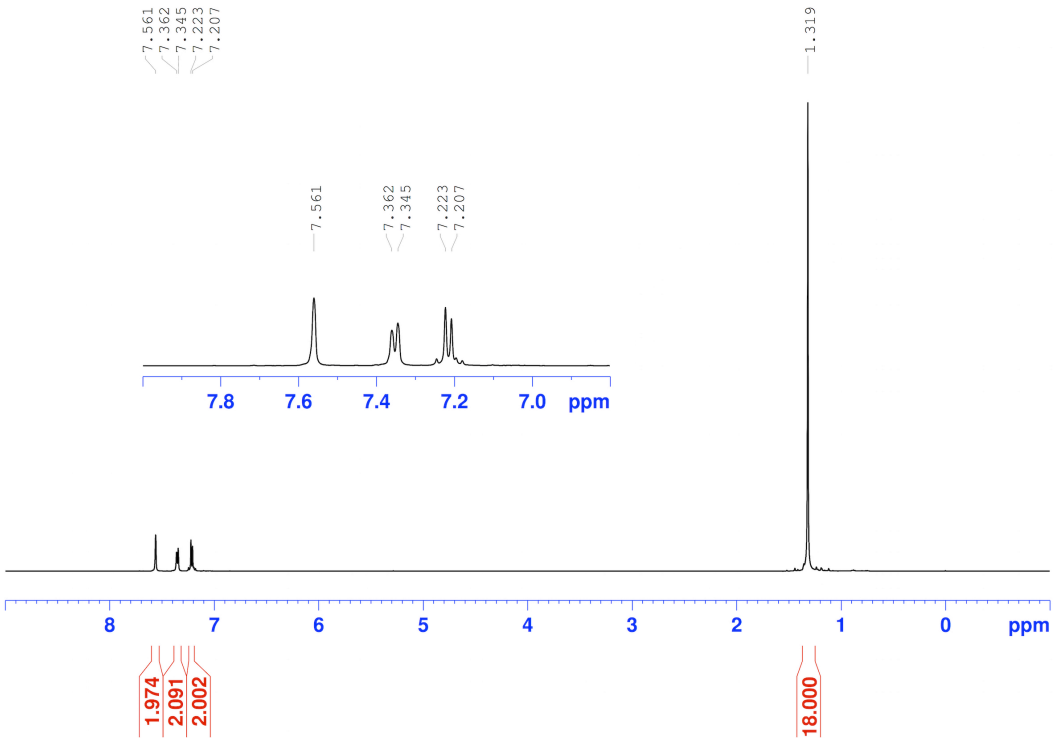

Fig. S6. ^{1}H NMR spectrum (500 MHz) of $\mathbf{1_{tBu}}$ in $CDCl_3$ at 25 °C.

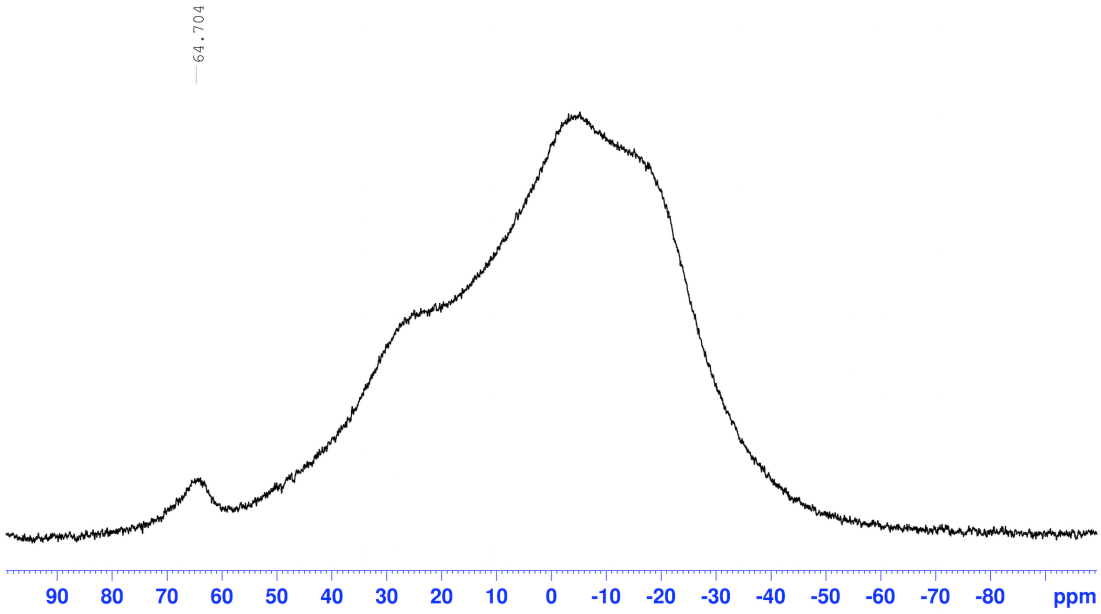

Fig. S7. ^{11}B NMR spectrum (128 MHz) of $\mathbf{1_{tBu}}$ in $CDCl_3$ at 25 °C. The broad peaks in a region from 50 to –40 ppm are the contributions from a borosilicate-glass NMR tube.

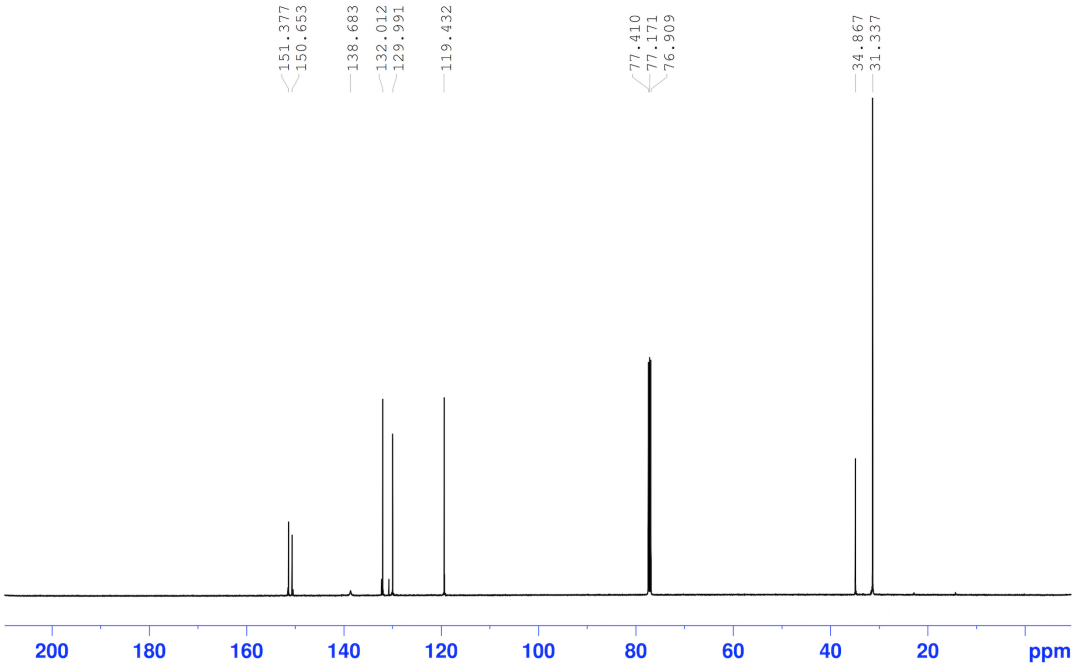

Fig. S8. ^{13}C NMR spectrum (125 MHz) of $\mathbf{1_{tBu}}$ in $CDCl_3$ at 25 °C.

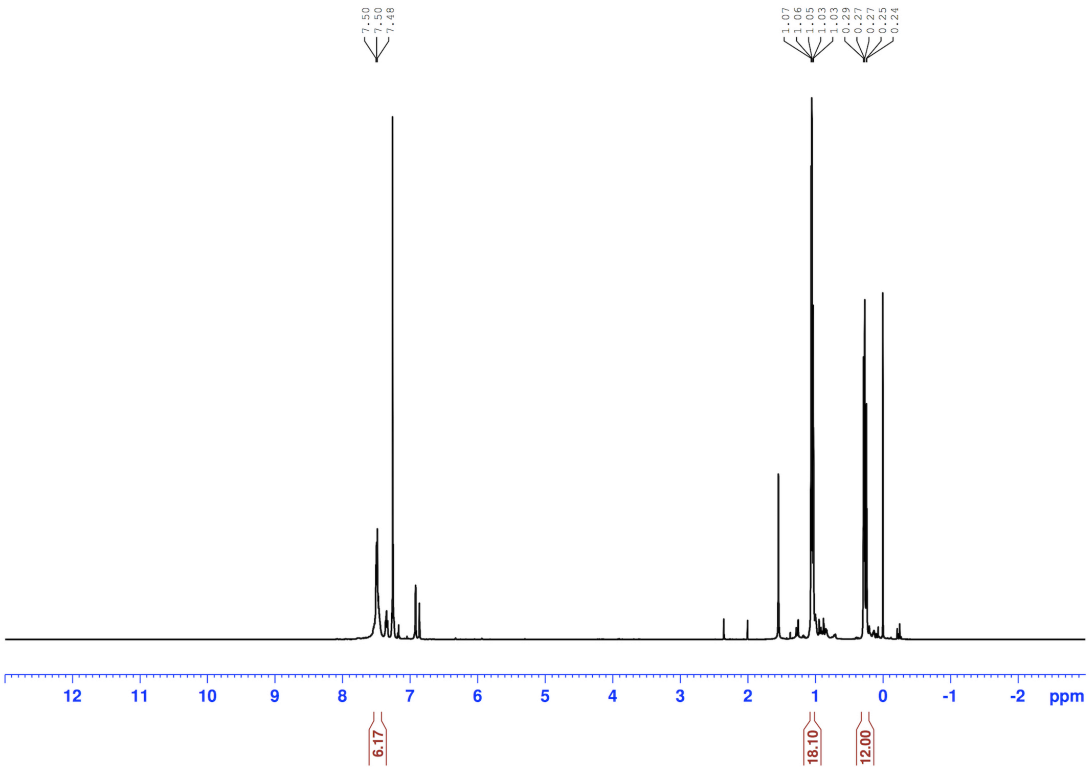

Fig. S9. ^{1}H NMR spectrum (500 MHz) of poly-$\mathbf{1_{OTBS}}$ in $CDCl_3$ at 25 °C.

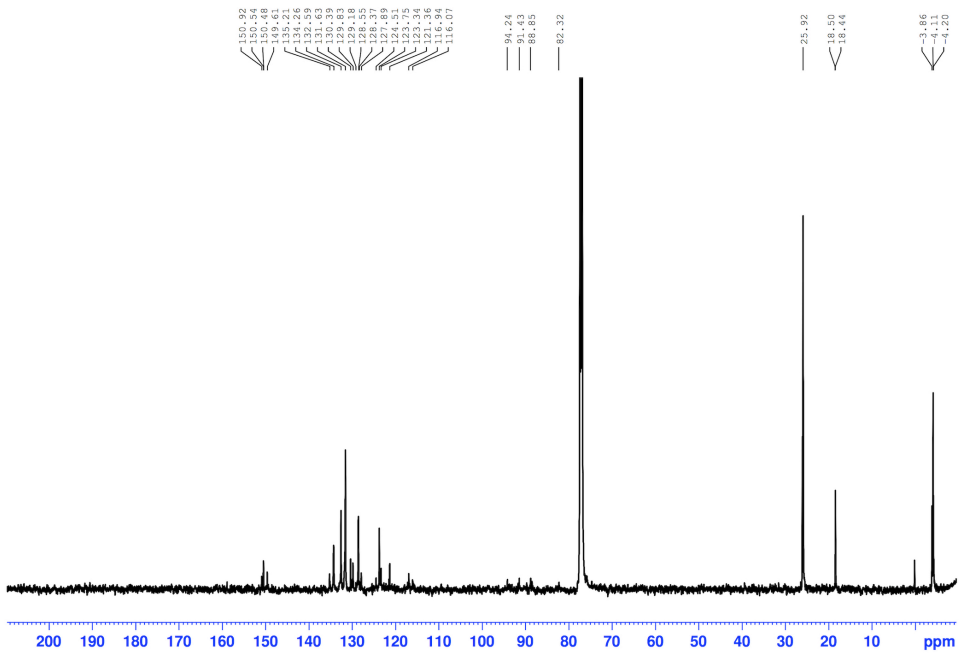

Fig. S10. ^{13}C NMR spectrum (125 MHz) of poly-$\mathbf{1_{OHex}}$ in $CDCl_3$ at 25 °C.

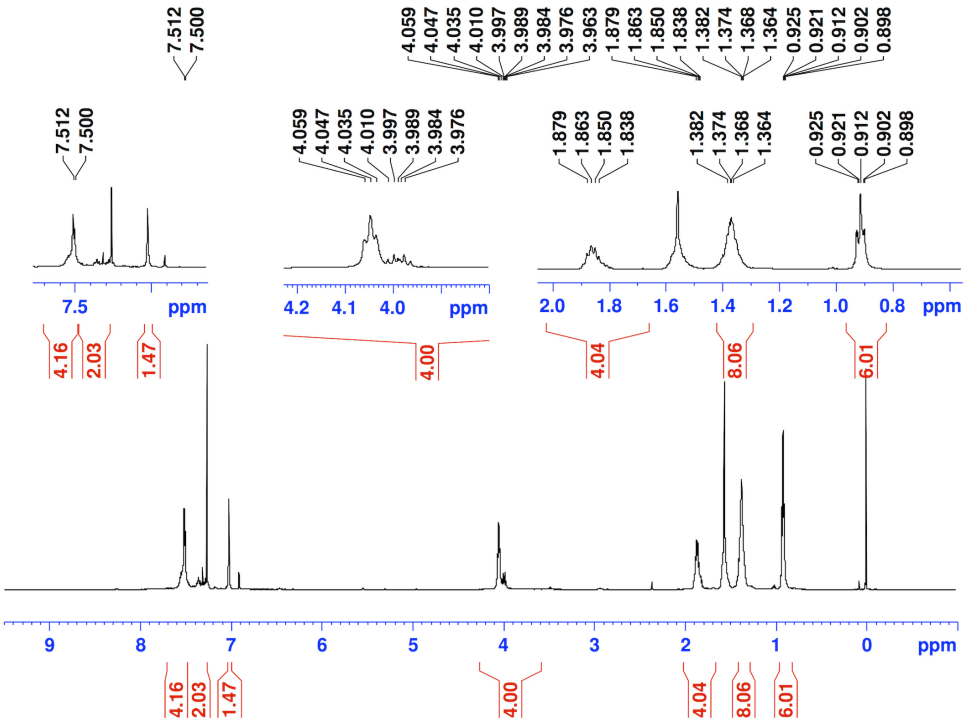

Fig. S11. ^{1}H NMR spectrum (500 MHz) of poly-$\mathbf{1_{OHex}}$ in $CDCl_3$ at 25 °C.

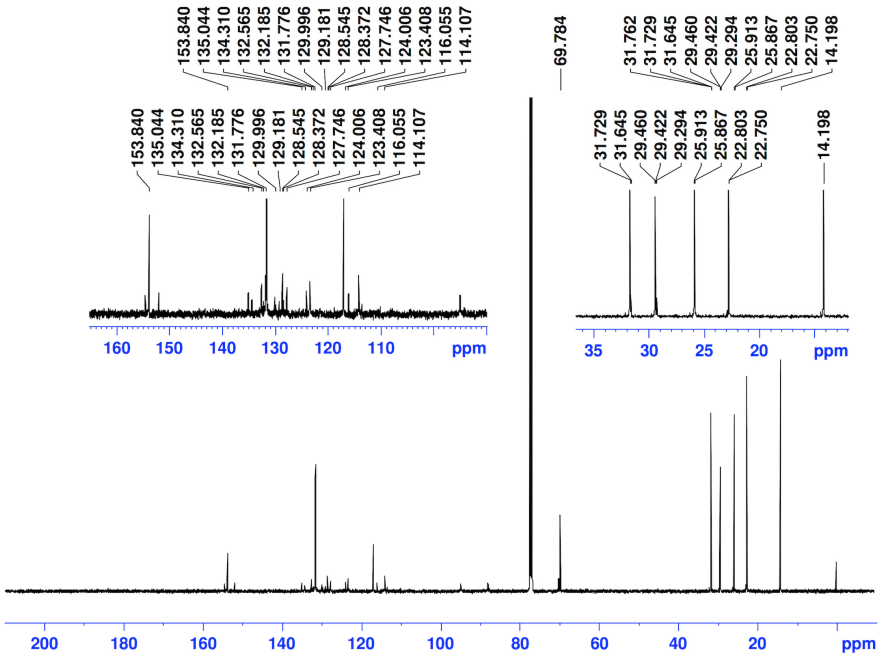

Fig. S12. ^{13}C NMR spectrum (125 MHz) of poly-$\mathbf{1}_{\mathbf{OHex}}$ in $CDCl_3$ at 25 °C.

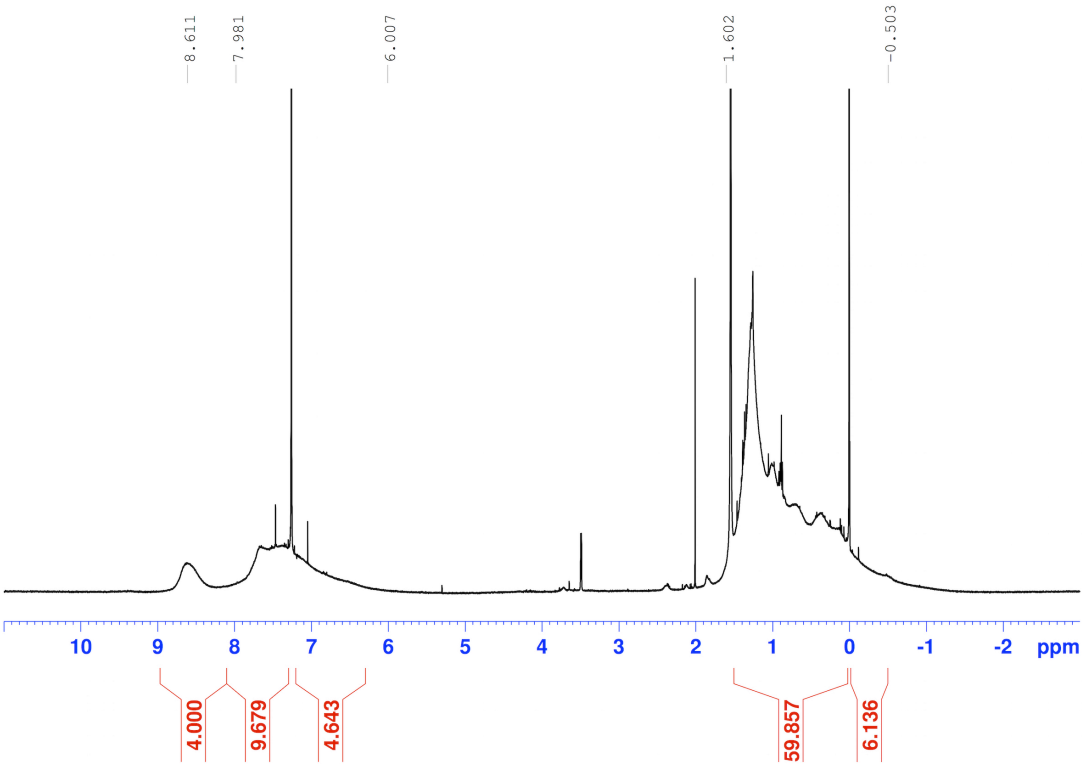

Fig. S13. ^{1}H NMR spectrum (500 MHz) of poly-$\mathbf{3}_{\mathbf{OTBS}}$-$^{t}\mathbf{Bu}_{\mathbf{100}}$ in $CDCl_3$ at 25 °C.

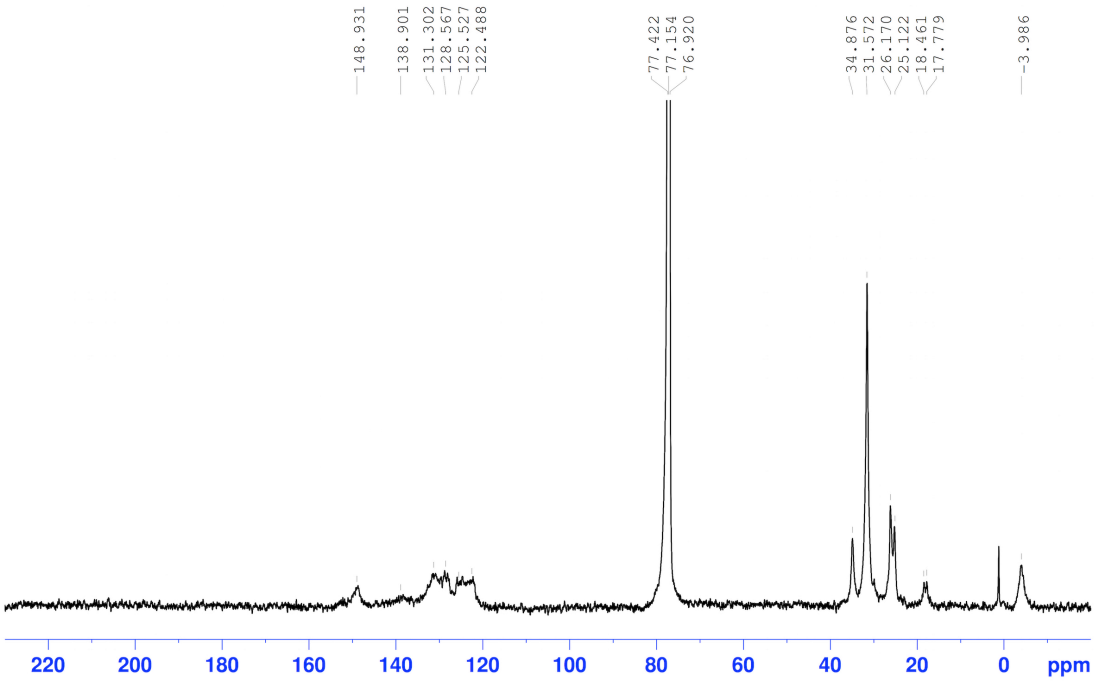

Fig. S14. ^{13}C NMR spectrum (125 MHz) of poly-**3**$_{\mathbf{OTBS}}$-^{t}**Bu**$_{\mathbf{100}}$ in $CDCl_3$ at 25 °C.

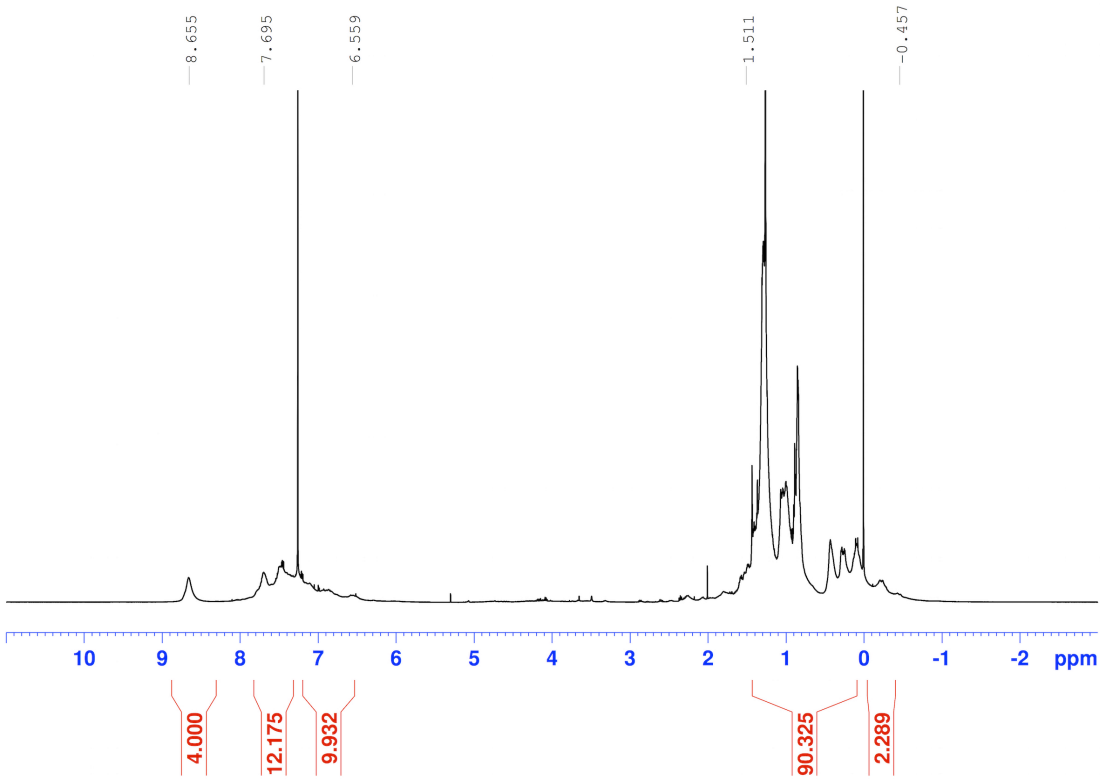

Fig. S15. ^{1}H NMR spectrum (500 MHz) of poly-**3**$_{\mathbf{OTBS}}$-^{t}**Bu**$_{\mathbf{50}}$ in $CDCl_3$ at 25 °C.

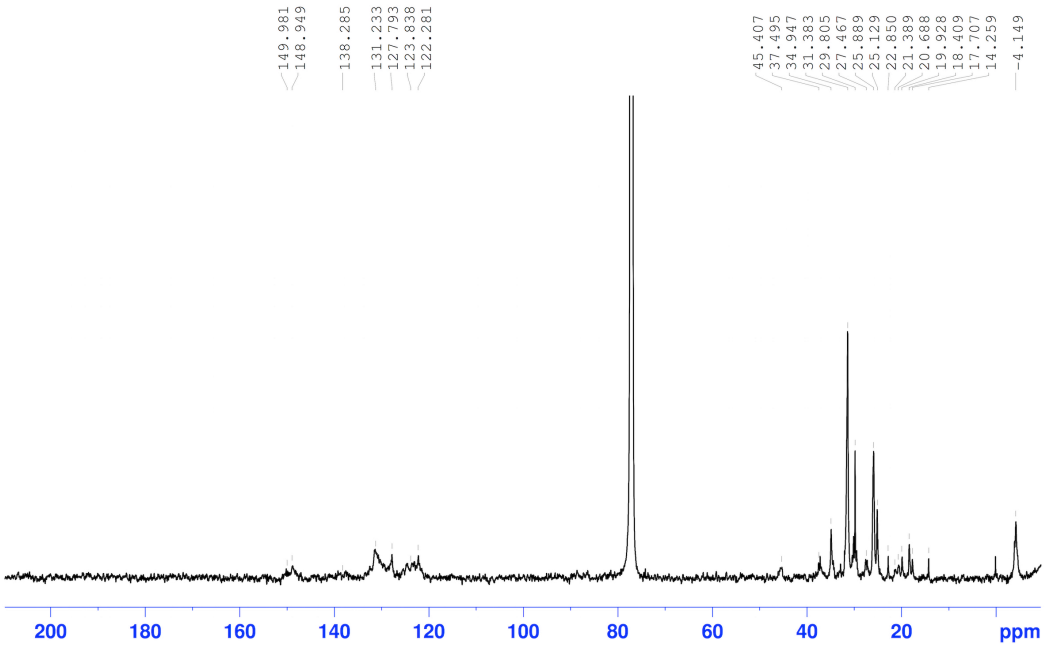

Fig. S16. ^{13}C NMR spectrum (125 MHz) of poly-$\mathbf{3_{OTBS}}$-$^{t}\mathbf{Bu_{50}}$ in $CDCl_3$ at 25 °C.

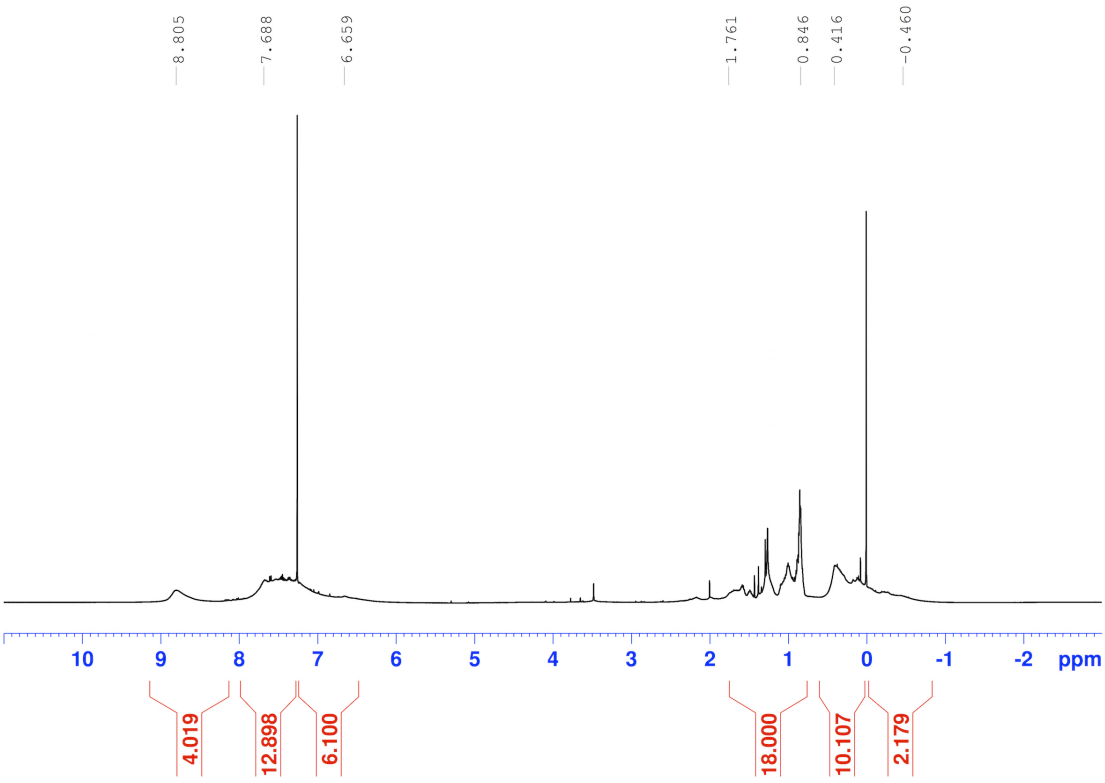

Fig. S17. ^{1}H NMR spectrum (500 MHz) of poly-$\mathbf{3_{OTBS}}$-$\mathbf{H_{100}}$ in $CDCl_3$ at 25 °C.

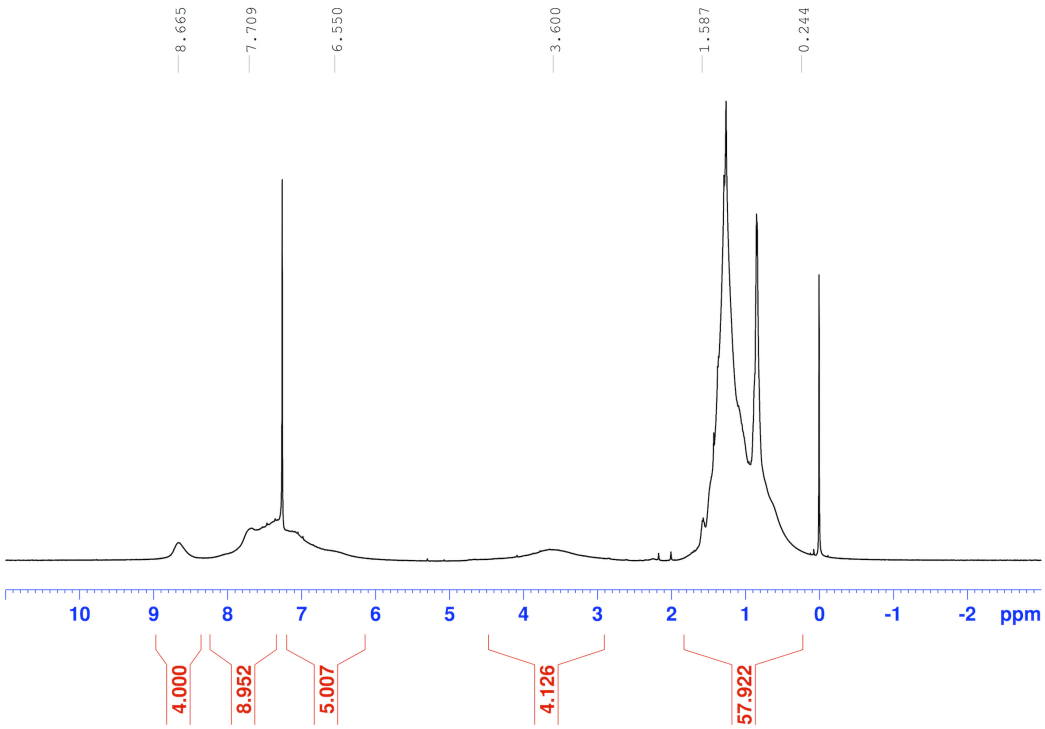

Fig. S18. ^{1}H NMR spectrum (500 MHz) of poly-**3**$_{\mathbf{OHex}}$-^{t}**Bu**$_{\mathbf{100}}$ in $CDCl_3$ at 25 °C.

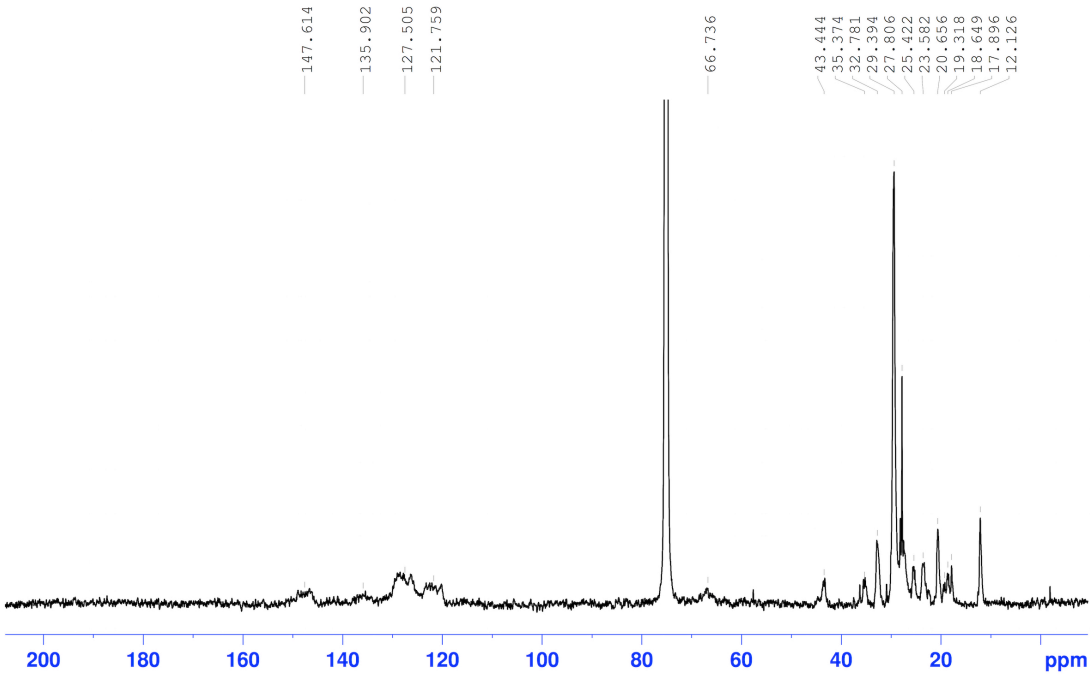

Fig. S19. ^{13}C NMR spectrum (125 MHz) of poly-**3**$_{\mathbf{OHex}}$-^{t}**Bu**$_{\mathbf{100}}$ in $CDCl_3$ at 25 °C.

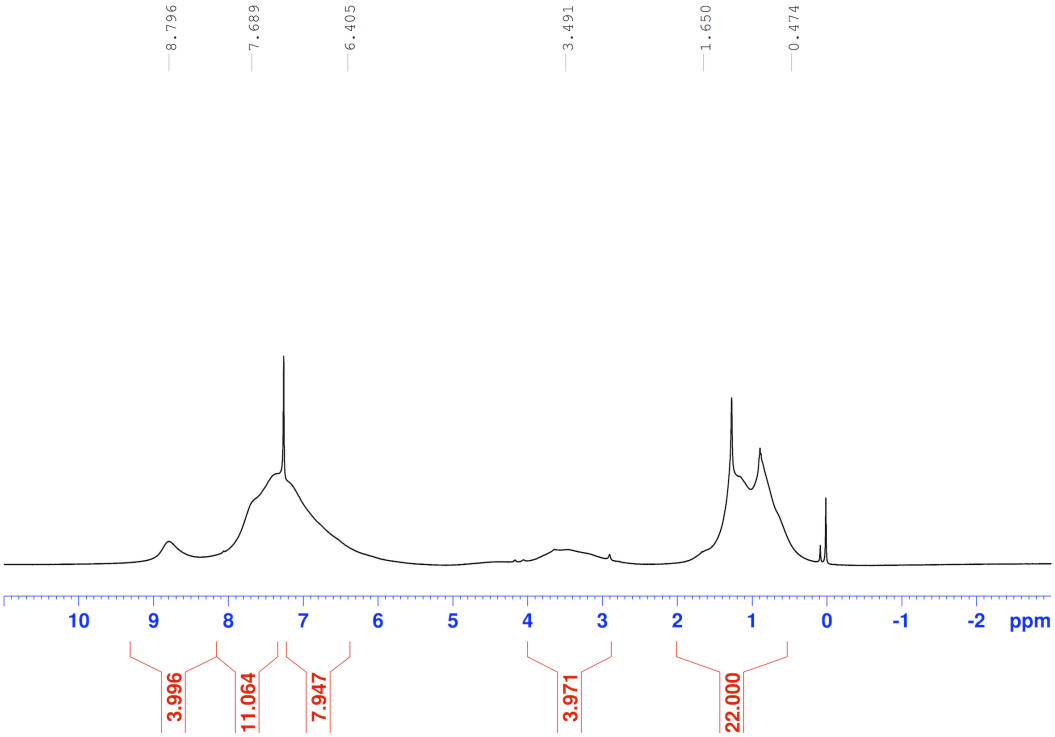

Fig. S20. ^{1}H NMR spectrum (500 MHz) of poly-$\mathbf{3_{OHex}}$-$\mathbf{H_{100}}$ in $CDCl_3$ at 25 °C.

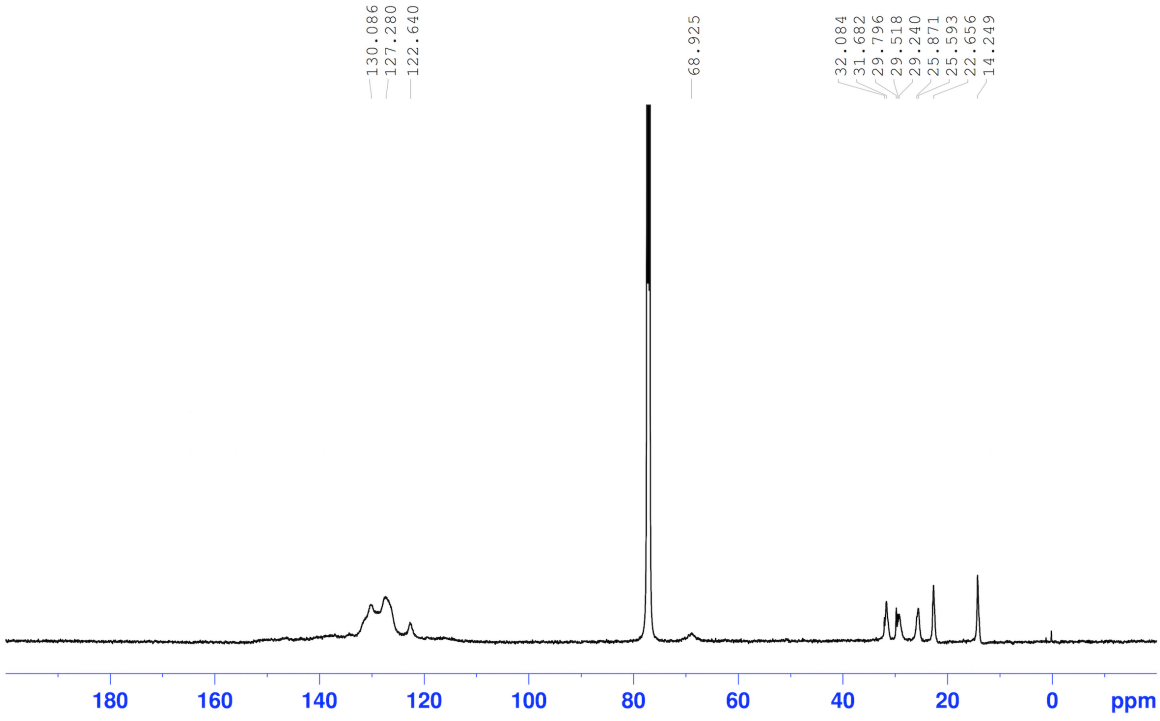

Fig. S21. ^{13}C NMR spectrum (125 MHz) of poly-$\mathbf{3_{OHex}}$-$\mathbf{H_{100}}$ in $CDCl_3$ at 25 °C.

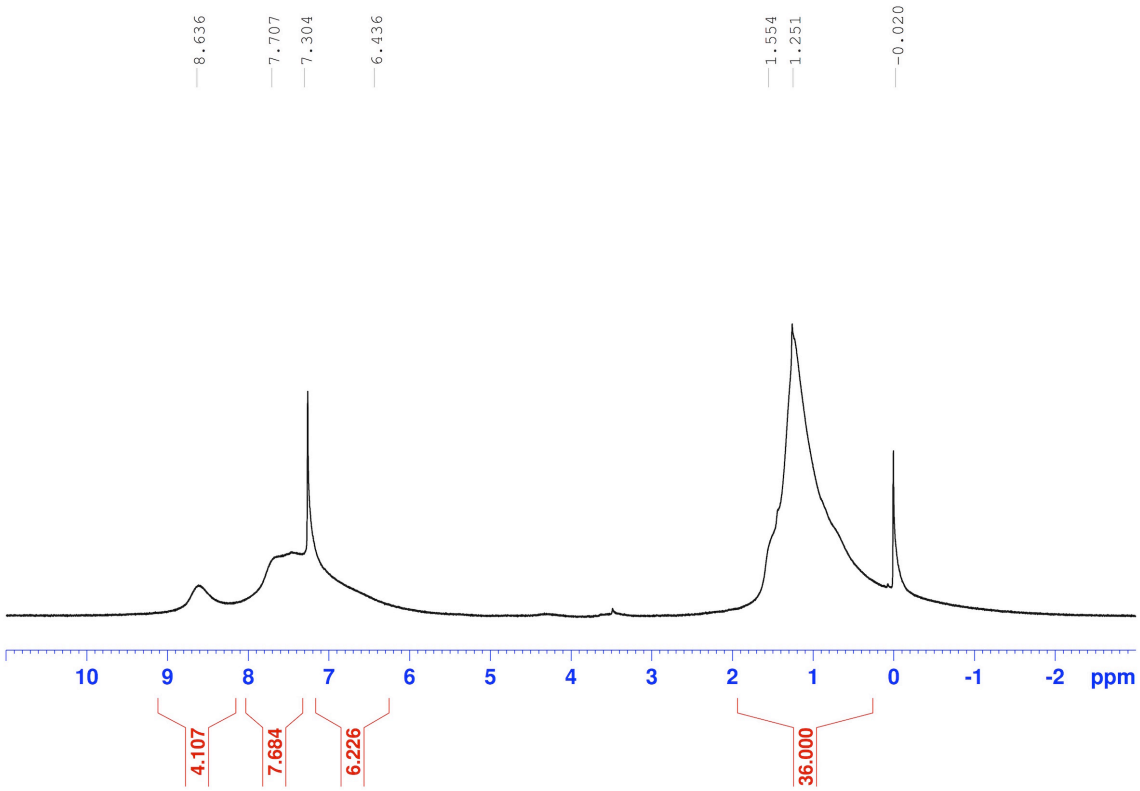

Fig. S22. ^{1}H NMR spectrum (500 MHz) of poly-$\mathbf{3_{OH}}$-$^{t}\mathbf{Bu_{100}}$ in $CDCl_3$ at 25 °C.

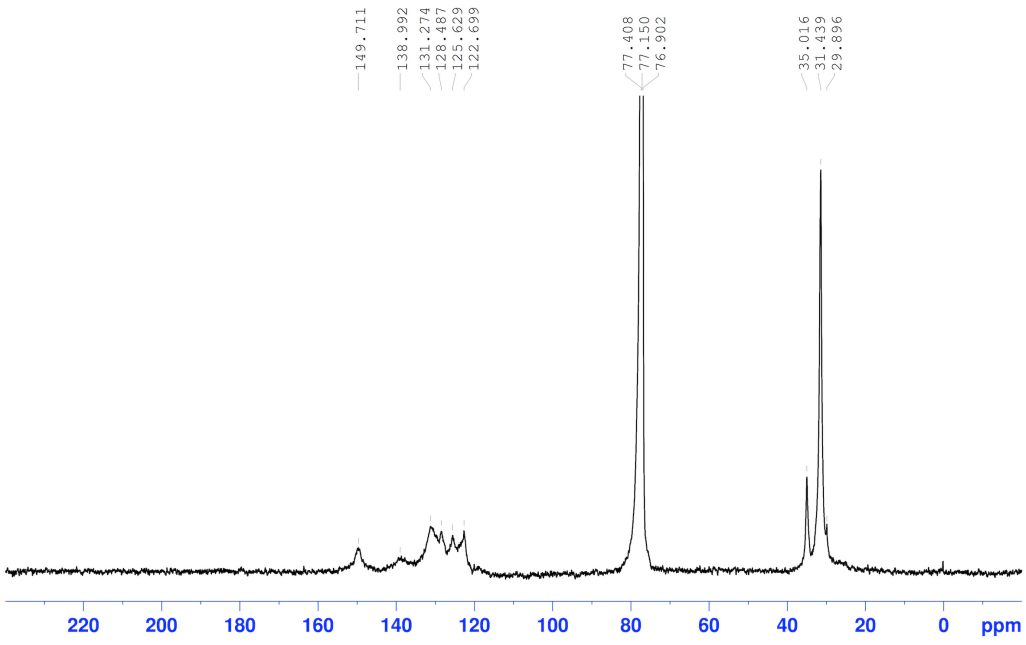

Fig. S23. ^{13}C NMR spectrum (125 MHz) of poly-$\mathbf{3_{OH}}$-$^{t}\mathbf{Bu_{100}}$ in $CDCl_3$ at 25 °C.